AIMS Biophysics

http://www.aimspress.com/journal/biophysics/

AIMS Biophysics, 11(1): 18–30.
DOI: 10.3934/biophy.2024002
Received: 10 September 2023
Revised: 19 November 2023
Accepted: 26 November 2023
Published: 10 January 2024

Letter

Rigidity sensing by blood-borne leukocytes: Is it independent of internal signaling?

Alireza Sarvestami[1,*], Madeline Smith[2], Arsha Moorthy[2], Patrick Kho[1], Lauren Talbo[1] and Chamaree de Silva[2]

[1] School of Engineering, Mercer University, Macon, GA 31207, USA
[2] College of Liberal Arts and Sciences, Mercer University, Macon, GA 31207, USA

* **Correspondence:** Email: sarvestani_a@mercer.edu; Tel: +14783012770.

Abstract: Atherosclerosis is a chronic inflammatory disease that results in the formation of lipid-rich lesions and stiffening of arterial walls. An increasing body of evidence suggests that nearly all members of the leukocyte family accumulate within atherosclerosis-prone arteries and participate in various stages of disease progression. Recently, it has been proposed that progressive changes of the elastic modulus of the arterial wall during plaque development may directly influence the kinematics of leukocyte rolling. In the present study, we propose that rigidity sensing of rolling leukocytes may occur spontaneously due to the stiffness-dependent elastic instability of reversible bonds between rolling leukocytes and the arterial walls. This effect is mechanistic in nature and operates independently of cell biochemical signaling. To partially test this hypothesis, we measured the rolling velocities of functionalized microparticles, comparable in size to leukocytes, interacting with E-selectin coated substrates of controlled stiffness. The kinematic analysis of the particles' motion reveals a larger rolling velocity on softer substrates, aligning with previous reports regarding monocytes. A simple kinetic model for a cluster of reversible bonds formed between a cell and the underlying substrate demonstrates that the critical forces needed for bond disassembly decrease as substrate stiffness decreases. Consequently, bonds are more likely to break on softer substrates, resulting in enhanced cell mobility.

Keywords: leukocyte rolling; atherosclerosis; rigidity sensing; flow chamber; bifurcation instability

1. Introduction

Leukocyte rolling on vascular endothelium is the key part of the immune surveillance response [1]. Adhesion of leukocytes to the apical surface of endothelial cells (ECs) is afforded by specific binding between selectins – a major family of EC receptors – and the oligosacharide moieties of ligands that

are constitutively expressed on the surface of leukocytes [2, 3]. Due to the reversible binding between ligands and receptors, leukocytes are captured by ECs and begin to roll on the vessel wall as directed by the hemodynamic flow. The chemistry of binding between selectin family members and their cognate ligands is extensively studied in the past. Activated ECs express E- and P-selectin at their luminal surface that recognize a range of distinct glycoconjugates present on leukocyte surface [4, 5]. ESL-1 and PSGL-1 are high-affinity ligands for E- and P-selectin receptors that are expressed on the surface of most circulating leukocytes [6–8]. For example, it is known that the C-type lectin domain of selectin binds to NH_2-terminal sLe^x-containing and a nearby tyrosine sulfate residue of PSGL-1 [9]. These specific bindings play a key role in leukocyte adhesion and rolling.

The crawling motility of some cells such as endothelial, fibroblasts and smooth muscle cells is known to be highly dependent on substrate stiffness [10, 11]. While still an open problem, the fundamentals of this phenomenon have been studied extensively [12, 13]. The rigidity sensing of blood-borne leukocytes, however, is not systematically examined in the past. Understanding how circulating leukocytes respond to the variation of substrate stiffness may reveal hitherto unknown aspects of leukocyte recruitment to atherosclerotic lesions [14]. The hallmarks of atherosclerosis are deposition of lipids at arterial walls followed by calcification and plaque accumulation through necrosis and fibrosis [15]. Homing and migration of leukocytes into the inflamed artery is an essential step in progression and growth of the atherosclerotic lesions. Recently, it has been proposed that enhanced recruitment of leukocytes might be caused by increased arterial stiffness. Vascular stiffness of atherosclerosis-prone artery can be increased to up to 100 kPa, significantly larger than that of a healthy artery [16]. Mackay and Hammer [17] measured the rolling velocity and capturing efficiency of monocytes in a creeping flow regime on soft substrates coated with selectin. Their measurements revealed a direct correlation between the rolling velocity of monocytes and the stiffness of underlying substrate. Decreasing the stiffness of substrates coated with E-selectin at constant site density from 20 to 1 kPa led to a higher average rolling velocity of cells. In contrast, substrate stiffness had a minimal impact on cell kinematics when substrates were coated with P-selectin. The latter was attributed to the higher binding affinity between P-selectin and PSGL-1 amino terminus. However, how substrate stiffness regulates the kinematics of leukocytes in presence of E-selectin is yet to be determined.

In this contribution, we propose that rigidity sensing by leukocytes rolling on substrates coated with E-selectin could be a mechanical process, independent of cell internal signaling. To demonstrate this in vitro, we substitute leukocytes with polystyrene particles of comparable size ($\sim 10\ \mu$m) that are coated with PSGL-1. We use a novel flow chamber with controlled substrate stiffness for this purpose and measure the rolling velocity of microparticles perfused over hydrogel substrates coated with E-selectin. By comparing these recorded velocities to the findings of Mackay and Hammer [17] concerning monocytes, we show that PSGL-1 coated microparticles exhibit a similar sensitivity to the mechanical stiffness of the underlying substrate. We present a simple model for stability of the contact zone between a rolling cell and the underlying substrate. It is essential to emphasize that the primary objective of presenting this model is not to simulate the motion of a leukocyte rolling on a soft surface. Instead, we solely focus on the stability of bonds assembled at cell footprint. The model reveals that substrate stiffness controls the bifurcation instability of assembled bonds and therefore could be a mediator for rigidity sensing of rolling cells.

2. Materials and methods

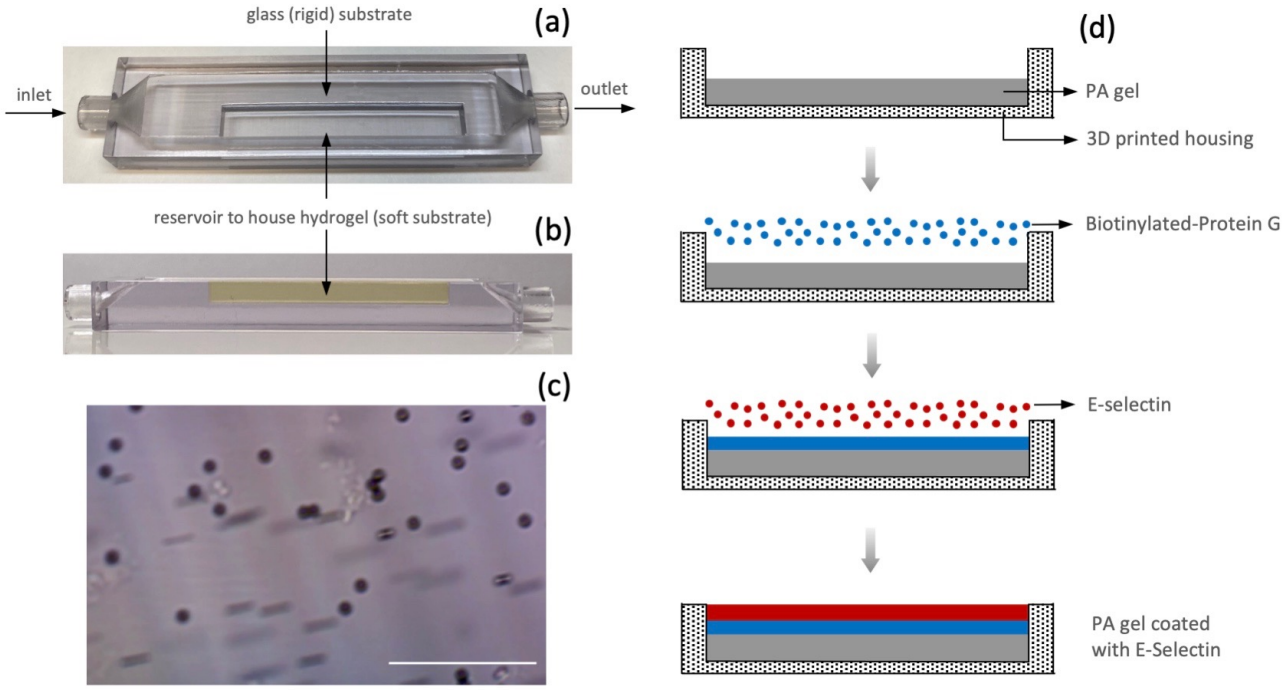

Figure 1. (a) Top and (b) side view of the custom-designed flow chamber. (c) A temporal snapshot of particles perfused in the flow chamber (scale bar: 100 μm). (d) Synthesis of PA gels with controlled stiffness coated with E-selectin receptors.

Synthesis of Gel: The chamber presents two different substrates with vastly different rigidities to the flowing particles (Figure 1). One side is made of the 3D printed resin, hereafter referred to as the rigid substrate. The other side is a reservoir filled with a polyacrylamide (PA) gel, hereafter referred to as the soft substrate. PA gels were polymerized with crosslinking of acrylamide and bis-acrylamide at different mass concentrations to make gels with a Young's modulus of 5, 10 and 20 kPa [18]. The polymerization was initiated by ammonium persulfate (APS) and tetramethylethylenediamine (TEMED) (Bio-Rad Laboratories) at a concentration of 0.1 % w/v. Gels were subsequently coated with recombinant human E-selectin–Fc chimeras (R&D Systems) (Figure 1). Selectin–Fc was conjugated to the gel surface using biotinylated-Protein G (ThermoFisher Scientific) [19]. Protein G was dissolved in PBS at a concentration of 20 μg/mL and added to the surface of the gels. Gels were incubated for 2 hr and then washed with PBS. E-selectin-Fc was dissolved in PBS at a concentration of 10 μg/mL and the solution was added to the surface of the gel. Gels were consequently incubated for 2 hr, rinsed gently with PBS and kept at 4 °C.

Preparation of Microspheres: Protein A-coated polystyrene beads (CP02 N, Bangs Labs) with a diameter of $\sim$ 10 μm were washed with PBS and subsequently centrifuged and separated from the supernatant. The washed particles were incubated with 100 μg/mL PSGL-1-Fc chimera solution (R&D Systems) for 2 hr at room temperature. After incubation, the particles were rinsed gently with PBS [19].

Parallel Plate Flow Chamber: The design process of the novel flow chamber used in this study is

explained in detail elsewhere [20]. In summary, the chamber was 3D printed with a stereolithography printer using a general purpose acrylic resin. The effective dimensions of the 3D printed chamber are $60 \times 10 \times 0.25$ mm. Two major design criteria were considered in determining the interior dimensions of the chamber: (1) achieving laminar flow under fully developed conditions and (2) preventing the sedimentation of flowing particles. To have a laminar flow, the Reynolds number, R_e, was set below 2,000 [21]. To ensure that the flow in the chamber is fully developed, the entrance length, l_e, was set equal to $l_e = 0.06R_eD$ with $D = 4A/P_w$, where A and P_w show the cross-sectional area of the chamber and its wetted perimeter, respectively [21]. If the flow is not sufficiently fast, the particles may sink due to their larger specific density compared to the surrounding fluid. To prevent sinking, the velocity of the particles in a laminar flow has to be sufficiently larger than the settling velocity. The terminal velocity of a single particle can be found using the Stokes' law

$$V_0 = \frac{d_p^2(\rho_p - \rho_m)g}{18\mu} \tag{2.1}$$

where g is the gravity acceleration, ρ_p is the particle's mass density, d_p is its diameter, ρ_m is the density of the fluid media and μ is the viscosity of the fluid. The settling velocity V_s of dilute suspensions in creeping motion can be obtained using Happel and Famularo's theory [22] for randomly dispersed spherical particles as

$$V_s = \frac{V_0}{1 + \gamma\phi^{1/3}} \tag{2.2}$$

where $\gamma = 1.30$ and ϕ is the volume fraction of particles in the media.

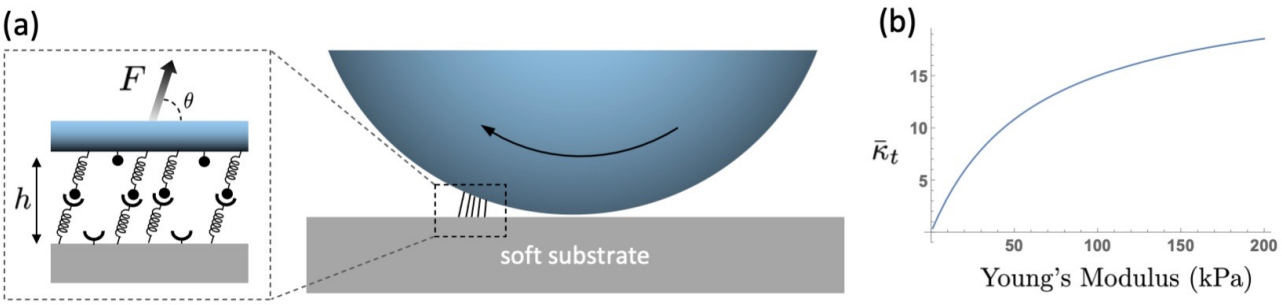

Figure 2. (a) As the rolling cell moves forward the ligand-receptor bonds at the cell footprint are strained. The complex geometry of the bonds is simplified by a cluster of N_b linear springs between the cell and substrate. The dividing gap distance between the surfaces is h and θ shows the angle between the tilted bonds and the underlying substrate. (b) Variation of (normalized) stiffness of the binding sites with the Young's modulus of the substrate, as indicated by Equations (2.7) and (2.8).

After in situ curing of the PA gel inside the chamber, it was cleaned and the excess amount of the gel was brushed off. A teflon film with an approximate thickness of 300 μm was placed between the top surface of the chamber and a coverslip. The assembly was tightly clamped to prevent leakage. The inlet tubing was connected to a syringe pump (Harvard Apparatus) for adjusting the flow rate and the outlet tubing to a reservoir. The chamber was placed on the stage of an inverted light microscope. The

shear stress generated by the flow, τ, must be within the range 50 – 200 mPa, comparable with the measured shear stresses in the post-capillary venules in vivo [23]. The required flow rate, Q, to reach the desired shear stress was calculated using

$$\tau = \frac{6\mu Q}{h_c^2 w} \tag{2.3}$$

where h_c is the effective height of the chamber (including the thickness of gasket). The experiments were conducted at a flow rate of 0.7 mL/min. Taking into account the chamber's effective dimensions, this flow rate results in a shear stress of 90 mPa. The fluid velocity $V = Q/h_c w$ was set to be greater than the settling velocity shown by Eq. (2.2). The beads suspended in distilled deionized water were perfused in the chamber at room temperature. A 10x phase objective was used to continuously monitor and record the beads motion. The trajectories were recorded and velocities were calculated using ImageJ.

Theoretical Model: Figure 2(a) schematically illustrates the contact zone between a rolling leukocyte and the underlying substrate. Reversible bonds form within this zone, which is significantly smaller than the cell size. These newly established bonds start stress-free and gradually stretch as the cell rolls forward and the gap distance h between the cell and substrate widens. Since this gap distance is significantly smaller than the cell radius, the contact zone may be regarded as two parallel rectangular plates [24]. The surface density of receptors on the top plate (cell) is presented as N_t/A where N_t stands for the total number of receptors and A is the area of the contact zone. The areal density of substrate ligands is denoted as c_l and is assumed to be substantially larger than the receptor density on the cell surface [25]. The plates are conjugated via N_b specific bonds, distributed across the area A. The bonds are oriented at angle θ with respect to the horizontal substrate. The binding kinetics between ligands and receptors can be expressed as

$$\frac{dN_b}{dA} = k_f c_l \frac{N_t - N_b}{A} - k_r \frac{N_b}{A} \tag{2.4}$$

where k_f and k_r are the binding and unbinding rates between ligands and receptors, respectively. At steady-state, $dN_b/dA = 0$ and [26]

$$\frac{k_f}{k_r} = K_{eq} \exp\Big[\frac{-\kappa_t (l_b - l_0)^2}{k_B T}\Big] \tag{2.5}$$

where $l_b = h/\sin\theta$ denotes the length of stretched bonds (Figure 2(a)), K_{eq} is the affinity, κ_t is the overall stiffness of each binding site, k_B is the Boltzmann constant and T is the absolute temperature.

Mechanical equilibrium dictates that the binding forces exerted by stretched bonds must balance the force F applied by the rolling cell on these bonds. We assume that the bonds function as linear springs with a rest length l_0. Therefore,

$$F = N_b \kappa_t \Big(l_b - l_0\Big) \tag{2.6}$$

The overall stiffness of binding sites, κ_t, can be estimated by considering two linear springs assembled in series: one representing the stiffness of each ligand-receptor bond, with spring constant κ_b and one showing the substrate stiffness with spring constant κ_s. This way

$$\kappa_t = \frac{\kappa_b \kappa_s}{\kappa_b + \kappa_s} \tag{2.7}$$

Note that κ_t could be smaller than κ_b if the substrate stiffness is sufficiently low (Figure 2(b)).

The deformation of a linear elastic half-space in response to a point force applied on the surface can be determined using the well-known Boussinesq solution in linear elasticity [27]. This solution exhibits singularity precisely at the location where the force is applied. One way to overcome this singularity is to replace the point force with a uniform traction distributed over a small circular area, $\mathcal{A}$, around the point where the force is applied. Using this method, Walcott and Sun derived a closed-form relationship between the resultant force and the average displacement under $\mathcal{A}$ [28]. Accordingly, κ_s was evaluated as

$$\kappa_s \approx \frac{4\pi}{7} \frac{rE}{(1+\nu)(1-\alpha\nu)} \tag{2.8}$$

where r is the radius of $\mathcal{A}$, E is the Young's modulus, ν is the Poisson's ratio of the elastic substrate and $1 < \alpha < 0.5$ is the bond orientation factor whose value depends on the angle between the point load and the substrate.

As the rolling cell moves forward, the binding force developed in the bonds increases. This force counterbalances the hydrodynamic forces applied on the cell by the viscous fluid [24]. The assembly of bonds becomes unstable at a sufficiently large binding force. To find this force, we conduct a simple stability analysis. The critical disassembly force is the bifurcation point, where the stable and unstable branches of the solution to equation (2.4) and (2.6) converge.

3. Results and discussion

Figure 3 presents the recorded flow velocities of PSGL-1 coated particles over substrates functionalized with E-selectin, normalized relative to the mean velocity on the control rigid substrates. It is evident that the rolling velocity of particles is sensitive to the variation of substrate stiffness. The results show that at a flow rate of 0.7 mL/min, the particle velocity decreases from approximately 12 to 4 μm/s as the substrate stiffness increases from 5 to 20 kPa. The free velocity of non-functionalized particles over non-adhesive substrates was measured to be around 25 μm/s. Although particle velocity on the control rigid side of the chamber is supposed to be independent of the stiffness of the soft side, the measurements revealed a slight reduction from around 5 to 3 μm/s as the gel stiffness on the soft side increases. This discrepancy suggests the presence of an error in experimental measurements, which can be attributed to the swelling behavior of the hydrogel. Swelling of hydrogels in aqueous media is a consequence of lower number density of the crosslink points. Therefore, the height of the flow pathway (h_c) is expected to decrease as the stiffness of the gel on the soft side decreases. While this error is present, its impact is expected to be relatively minor and does not significantly compromise the credibility of our experimental findings.

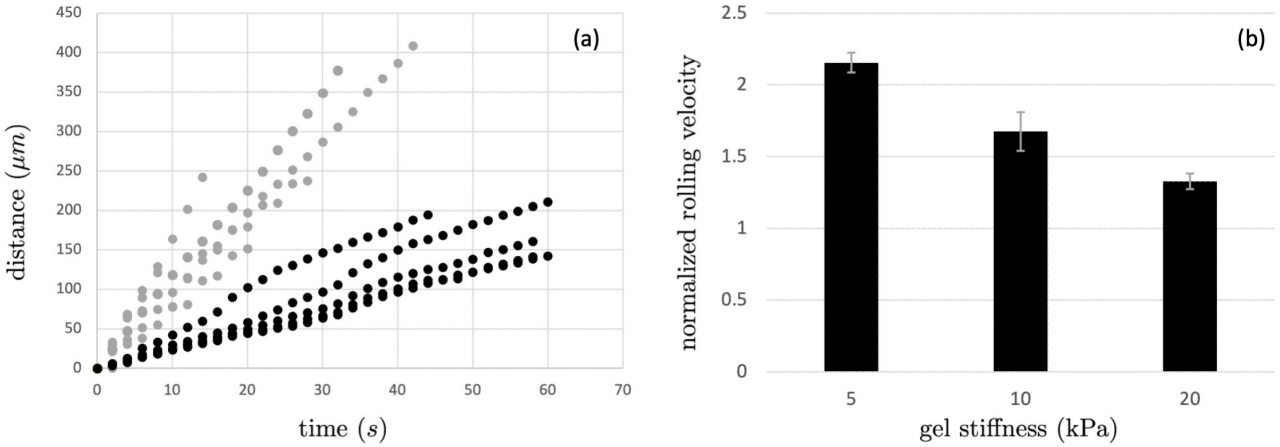

Figure 3. (a) Tracks of some representative particles on the 5 kPa (gray) and 20 kPa (black) substrates, plotted as distance traveled versus time. (b) Particle velocity over substrates functionalized with E-selectin at different substrate rigidities. The velocities are normalized relative to the mean velocity on the control rigid substrates. Error bars show the standard error of the mean. There was a statistically significant difference ($p < 0.01$) in rolling velocity relative to control.

The results shown by Figure 3 are qualitatively similar to those reported by MacKay and Hammer [17] for the rolling of monocytes on E-selectin coated hydrogels. This similarity hints that the mechanism underlying rigidity sensing in blood-borne leukocytes might be physical and independent of internal cell signaling pathways. In what follows, we leverage the insights gleaned from a stability analysis to propose a physical explanation for how leukocytes discern substrate stiffness.

Table 1. Model parameters.

Parameter	Definition	Range	Value	Reference
l_0	equilibrium length	$5 - 50$ nm	10 nm	[29]
κ_b	bond stiffness	$0.5 - 5$ pN/nm	1 pN/nm	[29]
K_{eq}	affinity	$10^7 - 10^{11}$ nm^2	10^8 nm^2	[29]
c_l	ligand density	$10^{-5} - 10^{-1}$ nm^{-2}	2.2×10^{-4} nm^{-2}	[29]
N_b	initial number of bonds		50	[29]
r	radius of $\mathcal{A}_f$		10 nm	[30]
α	bond orientation factor		0.5	[28]
ν	Poisson's ratio		0.5	[31]
T	temperature		310 K	

Table 1 lists the range and default values of model parameters. The ligand density is intentionally set at 2.2×10^{-4} nm^{-2}, resulting in the initial formation of 50 ligand-receptor bonds within the adhesion zone. This is comparable with the number of stress-free bonds in simulation results obtained by Hammer and Apte [29]. They employed adhesive dynamics, a computational algorithm to simulate the real-time motion of a spherical particle at proximity of an adhesive wall. Since the length of

stretched bonds is substantially smaller than the cell size, the bonds are all oriented nearly vertical relative to the substrate ($\theta \approx \pi/2$) [32]. This assumption leads to a bond orientation factor of 0.5. The substrate is assumed to be nearly incompressible with a Poisson's ratio of $\nu = 0.5$ [31].

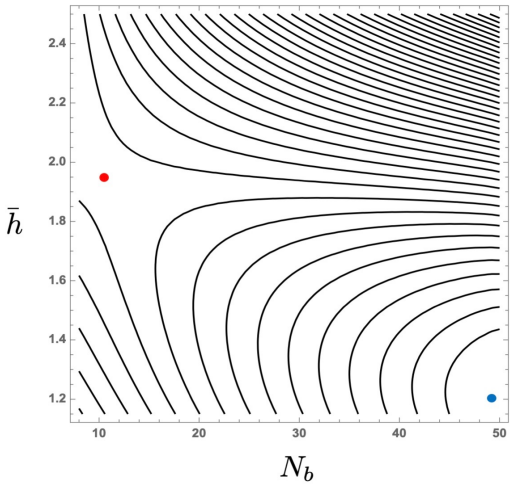

Figure 4. Two dimensional contour plots of the free energy variation as the number of bonds N_b and separation gap h change ($\bar{F} = 250$). The blue and red points show the local minima and saddle point solution, respectively ($\bar{\kappa}_t = 24.4$).

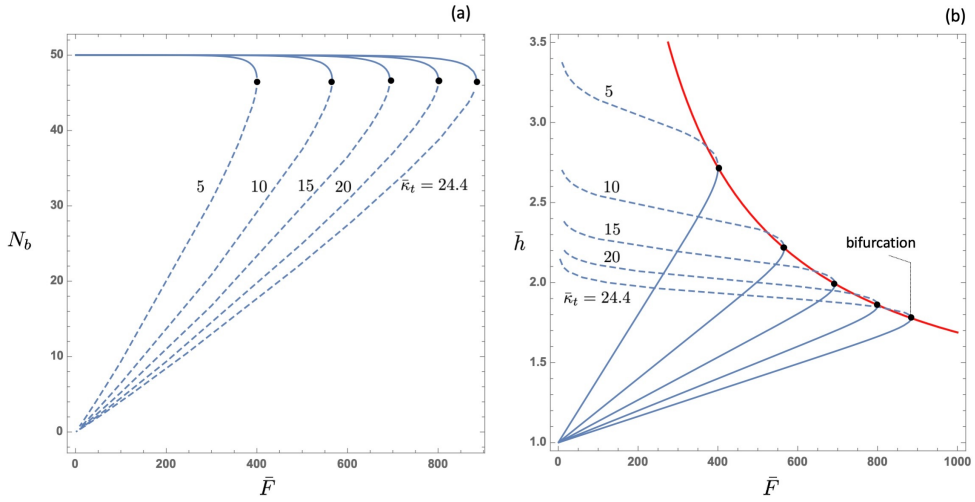

Figure 5. Variation of (a) the number of bonds N_b and (b) separation gap h with the binding force F at different binding stiffness κ_t. Stable and unstable solutions are on the solid and dashed-line branches, respectively. The bifurcation instability occurs at the intersection of stable and unstable branches, indicated by the red curve. Rigid substrates are characterized by $\bar{\kappa}_t = 24.4$.

The steady-state solution to equations (2.4) and (2.6) yields a stable (local minimum) and an unstable (saddle point) value at a given force F (Figure 4). The variation of the number of bonds in the adhesion zone (N_b) and normalized gap distance ($\bar{h} = h/l_0$) vs the normalized binding force ($\bar{F} = Fl_0/k_BT$) are shown in Figure 5. At a stress-free condition ($F = 0$), the adhesion zone is

comprised of 50 bonds. As the binding force increases, the number of bonds gradually decreases, concurrent with increasing the gap distance between the cell and the substrate. Continued tension leads to eventual disassembly of bond clusters due to a first-order saddle point bifurcation, where the stable and unstable branches of solutions intersect. As the substrate stiffness decreases, the total stiffness of each binding site ($\bar{\kappa}_t = \kappa_t l_b^2/k_B T$) decreases too (Figure 2(b)). Figure 5(b) further illustrates that the magnitude of the critical disassembly force at the bifurcation point decreases with $\bar{\kappa}_t$. This implies that clusters formed on softer substrates can support smaller forces and become unstable at lower tractions compared to bonds formed on stiffer substrates.

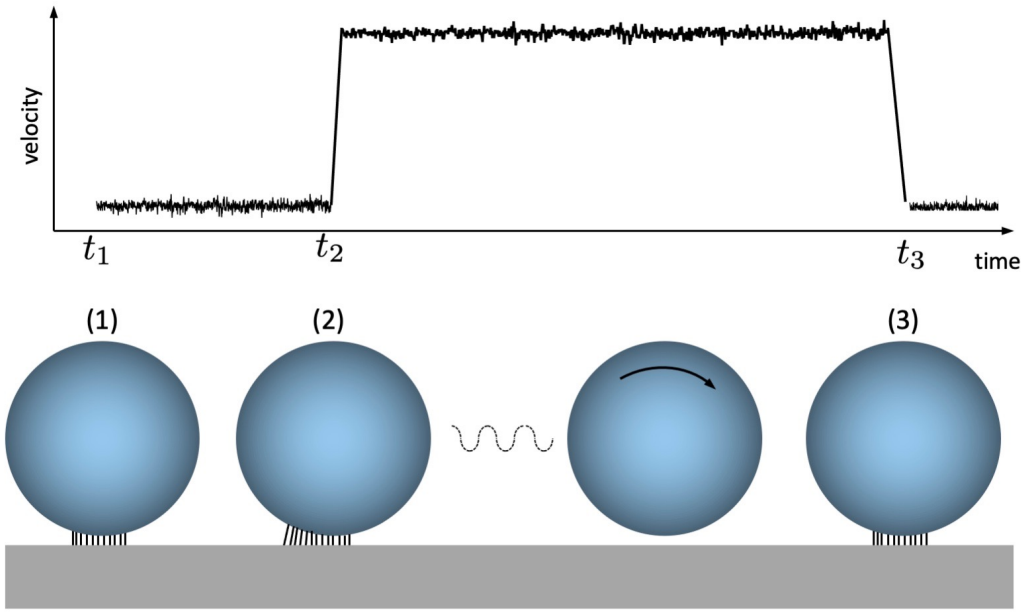

Figure 6. The leukocytes ability to discern substrate stiffness can be attributed to the elastic instability of established bonds between the cell and the substrate. When leukocytes roll along vascular endothelium, they undergo recurring sequences of arrest and release, mediated by selectin bonds that are established and ruptured during the short encounters between ECs and leukocytes. While the cell is only displaced slightly during the periods of arrest (between t_1 and t_2), its velocity experiences a sudden surge after the cluster of bonds are ruptured in face of dislodging hemodynamic forces. The instability of bonds on softer substrates amplifies the frequency of release events (between t_2 and t_3), leading to a greater average translational velocity.

The outcomes of this simple stability analysis present a feasible interpretation for how the substrate stiffness influences the rolling velocity of leukocytes. Leukocyte translocation on the endothelium displays a distinct pattern characterized by alternating periods of rapid movement and arrest [33]. This discrete pattern is schematically illustrated in Figure 6. A step-like movement happens when the bonds established in the footprint of the cell are ruptured. During the intervals between release events, the cell remains essentially at rest. During the arrest periods, the binding forces developed in bonds counterbalance the hydrodynamic forces and torques applied by the flowing media. When the molecular bonds are released, the cell is swiftly pushed forward to a new spot, where a balance between adhesive and hydrodynamic forces is restored. The stability analysis

presented here demonstrates that bifurcation instability occurs at smaller binding forces when the cell is attached to a softer substrate. Consequently, the frequency of release period increases, resulting in a higher average velocity of the cells. Accordingly, one could hypothesize that as the arterial wall stiffens, the residence time of attached cells increases, resulting in a reduction in the rolling velocity of these cells. Slower rolling and the potential arrest of leukocytes enhance the likelihood of transendothelial migration and their accumulation within lesions, as observed in atherosclerosis.

4. Conclusions

Following the pioneering study by Mackay and Hammer [17] on rolling adhesion of monocytes on soft substrates, we conducted a series of experiments to measure the rolling velocity of plastic microbeads coated with PSGL-1 on E-selectin coated hydrogels with different stiffness. Our findings reveal qualitative congruence with the experimental results of Mackay and Hammer. While our results do not preclude the possibility of active intracellular signaling, they introduce the intriguing prospect of a passive mechanism that potentially governs leukocyte rigidity sensing and operates independently of internal signaling pathways. In this model, the rigidity sensing is attributed to the stability of ligand-receptor bonds at the contact zone between the rolling cells and the substrate. We put forth a simple model for the stability of strained bonds established on compliant substrates. The results show that bifurcation instability has a close correlation with substrate stiffness. Specifically, it was found that the disassembly of bonds transpires at smaller forces as the substrate stiffness decreases. The instability and rupture of bonds formed on softer substrates lead to increased frequency of leukocyte translocation. It is important to note that our preliminary model exclusively addresses bond stability on compliant substrates and does not predict the kinematics of leukocyte rolling. For a precise simulation of leukocyte motion, it becomes crucial to assess the elasto-hydrodynamic interactions between the cell and its surroundings. Unlike beads, leukocytes are non-rigid entities that deform as they interact with the underlying substrate. This deformation not only alters the hydrodynamic forces experienced by the cell but also modifies the stiffness of equivalent springs, representing the local stiffness at each binding site. These modifications will be incorporated into more advanced studies in the future.

Use of AI tools declaration

The authors declare they have not used Artificial Intelligence (AI) tools in the creation of this article.

Acknowledgments

This work was supported by the seed grant provided by the Provost's office at Mercer University .

Conflict of interest

The authors declare no conflict of interests.

References

1. Ley K (2013) *Physiology of Inflammation*, New York: Springer. https://doi.org/10.1007/978-1-4614-7512-5
2. McEver RP (1994) Selectins. *Curr Opin Immunol* 6: 75–84. https://doi.org/10.1016/0952-7915(94)90037-X
3. Patel KD, Cuvelier SL, Wiehler S (2002) Selectins: critical mediators of leukocyte recruitment. *Semin Immunol* 14: 73–81. https://doi.org/10.1006/smim.2001.0344
4. Varki A (1994) Selectin ligands. *Proc Natl Acad Sci* 91: 7390–7397. https://doi.org/10.1073/pnas.91.16.7390
5. Rosen SD, Bertozzi CR (1994) The selectins and their ligands. *Curr Opin Cell Biol* 6: 663–673. https://doi.org/10.1016/0955-0674(94)90092-2
6. Zarbockn A, Müller H, Kuwano Y, et al. (2009) Psgl-1-dependent myeloid leukocyte activation. *J Leukocyte Biol* 86: 1119–1124. https://doi.org/10.1189/jlb.0209117
7. Carlow DA, Gossens K, Naus S, et al. (2009) Psgl-1 function in immunity and steady state homeostasis. *Immunol Rev* 230: 75–96. https://doi.org/10.1111/j.1600-065X.2009.00797.x
8. Zarbock A, Ley K, McEver RP, et al. (2011) Leukocyte ligands for endothelial selectins: specialized glycoconjugates that mediate rolling and signaling under flow. *Blood* 118: 6743–675. https://doi.org/10.1182/blood-2011-07-343566
9. McEver RP, Cummings RD (1997) Perspectives series: cell adhesion in vascular biology. role of psgl-1 binding to selectins in leukocyte recruitment. *J Clin Invest* 100: 485–491. https://doi.org/10.1172/jci119556
10. Lo CM, Wang HB, Dembo M, et al. (2000) Cell movement is guided by the rigidity of the substrate. *Biophys J* 79: 144–152. https://doi.org/10.1016/S0006-3495(00)76279-5
11. Yeung T, Georges PC, Flanagan LA, et al. (2005) Effects of substrate stiffness on cell morphology, cytoskeletal structure, and adhesion. *Cell Motil Cytoskel* 60: 24–34. https://doi.org/10.1002/cm.20041
12. Giannone G, Sheetz MP (2006) Substrate rigidity and force define form through tyrosine phosphatase and kinase pathways. *Trends Cell Biol* 16: 213–223. https://doi.org/10.1016/j.tcb.2006.02.005
13. Sheetz M (2019) A tale of two states: normal and transformed, with and without rigidity sensing. *Annu Rev Cell Dev Biol* 35: 169–190. https://doi.org/10.1146/annurev-cellbio-100818-125227
14. Eriksson EE (2003) Leukocyte recruitment to atherosclerotic lesions, a complex web of dynamic cellular and molecular interactions. *Curr Drug Targets Cardiovasc Hematol Disord* 3: 309–325. https://doi.org/10.2174/1568006033481357
15. Libby P, Ridker PM, Maseri A (2002) Inflammation and atherosclerosis. *Circulation* 105: 1135–1143. https://doi.org/10.1146/annurev.pathol.1.110304.100100
16. Sharif AR, Shadpour MT, Avolio A (2019) Progressive changes of elastic moduli of arterial wall and atherosclerotic plaque components during plaque development in human coronary arteries. *Med Biol Eng Comput* 57: 731–740. https://doi.org/10.1007/s11517-018-1910-4

17. MacKay JL, Hammer DA (2016) Stiff substrates enhance monocytic cell capture through e-selectin but not p-selectin. *Integr Biol* 8: 62–72. https://doi.org/10.1039/c5ib00199d

18. Tse JR, Engler AJ (2010) Preparation of hydrogel substrates with tunable mechanical properties. *Curr protoc Vell Biol* 47: 10–16. https://doi.org/10.1002/0471143030.cb1016s47

19. Farzi B, Young D, Scrimgeour J, et al. (2019) Mechanical properties of p-selectin psgl-1 bonds. *Colloid Surface B* 173: 529–538. https://doi.org/10.1016/j.colsurfb.2018.10.017

20. Chester B, de Silva C, Judd M, et al. (2022) Capstone project–design of a novel flow chamber to study the effects of vascular stiffness on migration of blood-borne cells. *In Proceeding of the American Society for Engineering Education* Charleston, SC. https://sites.asee.org/se/wp-content/uploads/sites/56/2022/03/2022ASEESE75.pdf

21. Athanasiou K, Natoli R (2009) *Introduction to Continuum Biomechanics*, Springer Cham. https://doi.org/10.1007/978-3-031-01626-4

22. Famularo J, Happel J (1965) Sedimentation of dilute suspensions in creeping motion. *AIChE J* 11: 981–988. https://doi.org/10.1002/aic.690110608

23. Slack SM, Cui Y, Turitto VT (1993) The effects of flow on blood coagulation and thrombosis. *Thromb Haemost* 70: 129–134. https://doi.org/10.1055/s-0038-1646173

24. Krasik EF, Hammer DA (2004) A semianalytic model of leukocyte rolling. *Biophys J* 87: 2919–2930. https://doi.org/10.1529/biophysj.104.039693

25. Kuo SC, Hammer DA, Lauffenburger DA (1997) Simulation of detachment of specifically bound particles from surfaces by shear flow. *Biophys J* 73: 517–531. https://doi.org/10.1016/s0006-3495(97)78090-1

26. Dembo M, Torney DC, Saxman K, et al. (1988) The reaction-limited kinetics of membrane-to-surface adhesion and detachment. *Proc R Soc London B Biol Sci* 234: 55–83. https://doi.org/10.1098/rspb.1988.0038

27. Johnson KL, Johnson KL (1987) *Contact Mechanics*. Cambridge university press. https://doi.org/10.1017/CBO9781139171731

28. Walcott S, Sun SX (2010) A mechanical model of actin stress fiber formation and substrate elasticity sensing in adherent cells. *Biophys J* 107: 7757–7762. https://doi.org/10.1073/pnas.0912739107

29. Hammer DA, Apte SM (1992) Simulation of cell rolling and adhesion on surfaces in shear flow: general results and analysis of selectin-mediated neutrophil adhesion. *Biophys J* 63: 35–57. https://doi.org/10.1016/s0006-3495(92)81577-1

30. Huang JY, Peng XL, Xiong CY, et al. (2011) Influence of substrate stiffness on cell–substrate interfacial adhesion and spreading: a mechano-chemical coupling model. *J Colloid Interf Sci* 355: 503–508. https://doi.org/10.1016/j.jcis.2010.12.055

31. Dimitriadis EK, Horkay F, Maresca J, et al. (2002) Determination of elastic moduli of thin layers of soft material using the atomic force microscope. *Biophys J* 82: 2798–2810. https://doi.org/10.1016/S0006-3495(02)75620-8

32. Chang KC, Hammer DA (1996) Influence of direction and type of applied force on the detachment of macromolecularly-bound particles from surfaces. *Langmuir* 12: 2271–2282. https://doi.org/10.1021/la950690y

33. Zhao YH, Chien S, Skalak R (1995) A stochastic model of leukocyte rolling. *Biophys J* 69: 1309–1320. https://doi.org/10.1016/s0006-3495(95)79998-2

AIMS Press